Received: 29 January 2024 | Revised: 26 September 2024 | Accepted: 3 November 2024

IET Renewable Power Generation

DOI: 10.1049/rpg2.13161

The Institution of Engineering and Technology WILEY

ORIGINAL RESEARCH

Distributed multi-layer control of hybrid AC/DC grids: Design and experimental validation

Riccardo Lazzari[1] | **Alessio La Bella**[2]

[1]Materials and Generation Technologies Department, RSE SpA, Milan, Italy

[2]Dipartimento di Elettronica, Informazione e Bioingegneria, Politecnico di Milano, Politecnico di Milano, Milan, Italy

Correspondence
Riccardo Lazzari, Materials and Generation Technologies Department, RSE SpA, Milan, Italy.
Email: riccardo.lazzari@rse-web.it

Abstract

As the electrical system becomes more and more decentralized, new control algorithms are necessary to manage the intermittent and non-deterministic production of non-programmable renewable sources, as well as the consumption of new loads like electric vehicles and heat pumps. Traditionally, electrical networks are controlled centrally, which provides full controllability of the system but introduces issues on scalability and complexity. This paper proposes a distributed multilayer control scheme based on model predictive control (MPC) applied to different portions of an electrical grid, optimizing power exchanges for balancing services. The first layer comprises local decentralized MPC controllers managing their areas, while the high-level distributed supervisor layer coordinates the exchange of flexibility between the network areas by acting on AC/DC converters. The overall distributed control architecture is applied and experimentally validated through the distributed energy resources test facility of RSE, showing enhanced performances in terms of prompt control action and compensation of the power disturbances.

1 | INTRODUCTION

The diffusion of renewable energy sources (RES) has introduced challenges for a system originally designed to handle unidirectional power flows from major generation facilities connected through rotating electric machines to end-users. To facilitate the decentralization of the electricity system, it is necessary to explore, develop and test new coordination and control algorithms capable of accommodating the unpredictable and intermittent nature of renewable energy sources (RESs) and new electrical loads.

The development of such tools must consider the prospects of the electricity system, the development of intelligent distribution networks and the diffusion of novel technologies. The changes are, in fact, still ongoing and will lead to further developments in the coming years, such as the creation of hybrid AC/DC distribution networks, in which multi-terminal direct current networks connect multiple nodes of the AC distribution network through power electronics converters [1, 2]. The introduction of DC links into an AC network brings numerous advantages, such as the possibility of transferring power with higher efficiency [3], the controllability of the flows by acting on the interface converters [4] and greater transmission capacity [5, 6], guaranteeing a more secure supply of the service and avoiding network congestions [7–9]. Furthermore, it is believed that the availability of DC connections could facilitate the integration of distributed energy resources (DERs), which is essential for reducing the environmental impact [10]. However, the decentralization of the electricity system requires the adoption of new control infrastructures focusing on flexible resources to promptly restore active power imbalances [11].

The literature suggests centralized strategies to mitigate power variations in external loads and DERs by managing distributed generators, storage systems and microgrids [12]. The integration of flexible resources coupled with accurate forecasts of renewable source generation and load consumption, positions model predictive control (MPC) as the most promising control design method for this category of issues [13, 14]. While the use of centralised MPC regulators for balancing unforeseen power variations has been proposed [15, 16] the drawbacks of pure centralised approaches, including scalability and computational complexity issues, make them unsuitable for the efficient control of large-scale systems like modern hybrid AC/DC distribution networks. Effective methods to control large

systems involve the design of local controllers for each energy source coordinated through hierarchical, and multilayer structures, involving information exchange between local regulators and a coordinating supervisor [17, 18]. Nevertheless, hierarchical approaches depend on a time-scale separation between the control layers, which may not be well-suited for the real-time correction of power imbalances owing to the slower time rate of the high-level controller.

Alternatively, distributed control structures, wherein each energy resource can communicate with others, can be used to optimize the coordination of resources and achieve global goals [19, 20]. Although this approach avoids scalability issues and is suitable for large-scale systems, distributed algorithms often involve slow, iterative, and communication-intensive procedures necessary for agent coordination. Generally, as the time needed for these coordination procedures is variable and cannot be predetermined, distributed approaches may not be well-suited for promptly compensating power imbalances.

A solution to address scalability challenges in large networks involves dividing the grid into multiple areas and coordinating their operations. The decomposition of the distribution network into small-scale, non-overlapping sub-areas, denoted as clusters, represents a solution to reduce the perturbations of the network, minimize contingencies and favour the integration of renewable generation within the distribution network [21, 22]. The cluster is a portion of the grid which has one or more connection points with the main grid and the other clusters (AC or DC), generation and load systems and is equipped with its controller capable of locally compensating the variations in active power for the expected values while ensuring a reserve that can be used to provide further services to the network or adjacent clusters.

Given these premises, this paper aims to develop and experimentally validate a two-layer distributed control architecture for hybrid AC/DC grids divided into clusters to ensure stable and continuous operation of the system, reducing disturbances to the main network and, at the same time, minimizing network contingencies. The lower layer consists of MPC regulators to coordinate dispatchable generators and associated storage units within each cluster to address local demand variability. The upper layer involves a fully distributed optimization problem which is responsible for assisting clusters facing shortages by reallocating flexibility from others. The proposed architecture is tested on a real experimental facility at Ricerca sul Sistema Energetico—RSE SpA, comprising different generation, storage and load units, as well as the presence of hybrid AC/DC grids. This paper extends the above-mentioned preliminary works on the control of multi-area electrical grids. In particular, [21] considers a centralized supervisor without any experimental validation; [22] does not consider the presence of hybrid AC/DC grids and it is validated in simulation; finally, the derivation of the algorithm used to define a fully distributed control structure is missing in [23], and the proposed control architecture was not validated with a consistent experimental campaign, as the one discussed in Section 4.

The paper is organised as follows: In Section 2 the proposed distributed control architecture for active power balancing is presented. The experimental setup used to validate the control is described in Section 3 and the test results are reported in Section 4, where the control architecture is applied to the experimental setup. Finally, conclusions are drawn in Section 5.

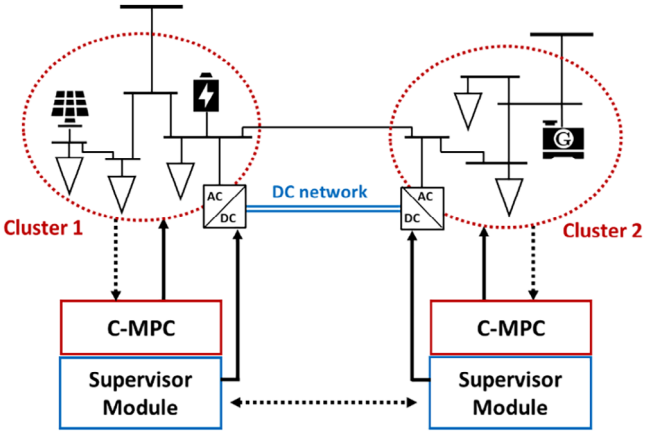

FIGURE 1 Schematic of the control scheme composed of local Cluster Model Predictive Controls (C-MPCs) and a distributed supervisor layer.

2 | PROPOSED CONTROL SCHEME

The proposed architecture has the aim of managing a hybrid AC/DC grid divided into clusters to compensate for the variability of non-programmable renewable energy sources and loads. In this way, the active power exchanged by each cluster with the rest of the grid is equal to the day-ahead program, despite the local variability caused by the RESs and from the loads. In the following, it is assumed that the clusters have already been properly created using one of the existing network partitioning algorithms, for example ref. [22].

The schematic of the overall architecture is presented in Figure 1. The first control level is constituted by a cluster model predictive control (C-MPC), designed for each cluster, and executed at each time step to compensate for the variability of the active power inside of individual clusters requesting balancing services from local dispatchable resources.

In case local power sources in a cluster are not able to balance the internal power variability, a power request is sent to the supervisor which provides a power dispatch solution among clusters through the resolution of an optimization problem executed immediately after running the C-MPCs. The goal is to support clusters that require power, directing it from those clusters that have it available by acting on the controllable interfaces of the multi-terminal DC grid which interconnects all the clusters. In this way, power is effectively transferred among different areas of the grid. The supervisor can be implemented either through a centralized structure [21] or by employing a fully distributed approach, providing advantages in terms of the control system's flexibility as explained in detail in the next sections.

2.1 | Cluster modelling

A cluster is a portion of the AC grid, where are present both dispatchable elements, such as batteries and controllable

generators, and non-dispatchable elements, like loads and RESs. Moreover, it is supposed that each cluster has an AC/DC interconnection point with the DC grid. The AC net active power $P_{\text{net},i}(t)$ of the ith cluster is defining as follows:

$$P_{\text{net},i}(t) = \sum_{k \in \aleph_i^D} P_{D,ki}(t) + \sum_{k \in \aleph_i^{\text{ND}}} P_{\text{ND},ki}(t) + P_{\text{DC},i}(t) \quad (1)$$

where $P_{D,ki}(t)$ is the power of the kth dispatchable unit of the ith cluster (e.g., a generator or a battery), $P_{\text{ND},ki}(t)$ is the power of the kth non-dispatchable element of the ith cluster and $P_{\text{DC},i}(t)$ is the power exchanged through the DC grid. Clusters aim to minimize the variation between their effective output power and the one dictated by the day-ahead scheduled profile. To achieve this objective, each cluster can use the reserve of power and energy of the dispatchable elements belonging to the cluster or it can require the necessary power and energy from other clusters. Thus, each ith cluster is characterized by the flexibility of the dispatchable elements, that is represented by an active power variation of the kth dispatchable element $\Delta P_{D,ki}(t)$ limited between an upper limit $R^{\uparrow}_{D,ki}(t)$ and a lower limit $R^{\downarrow}_{D,ki}(t)$:

$$R^{\downarrow}_{D,ki}(t) \leq \Delta P_{D,ki}(t) \leq R^{\uparrow}_{D,ki}(t) \quad (2)$$

As expressed in (2) the amount of power that can be provided is not constant, but it depends on the working condition of the dispatchable unit. Moreover, in the case of a battery, it is necessary to consider the amount of energy stored in the battery. Thus, it is possible to write the energy variation as expressed in (3) where the battery efficiency is neglected for simplicity:

$$\Delta E_{B,ki}(t+1) = \Delta E_{B,ki}(t) - \tau_s \Delta P_{B,ki}(t) \quad (3)$$

where $\Delta E_{B,ki}$ is the energy variation with respect to the day-ahead schedule, whereas τ_s is the sampling time. Thus, for the battery it is necessary to consider the energy reserves:

$$R^{\downarrow}_{E,ki}(t) \leq \Delta E_{B,ki}(t) \leq R^{\uparrow}_{E,ki}(t) \quad (4)$$

where $R^{\downarrow}_{E,ki}(t)$ and $R^{\uparrow}_{E,ki}(t)$ are the lower and upper limit of the energy reserve, dynamically depending on the stored energy.

2.2 | Cluster MPC

The first level of control is implemented in each cluster and acts periodically to compensate for the active power variability within the clusters due to unexpected variations of RESs or loads, expressed in (5). To do this, the C-MPC varies the power of the dispatchable resources, considering the constraints expressed in (2)–(4). Furthermore, the C-MPC is designed to send support requests to the higher level, that is, the supervisor, when for example, the local sources do not have enough reserves to satisfy the variability of loads/RESs within the cluster.

As anticipated, the C-MPC system is based on the model predictive control (MPC) technique, which provides for the solution of an optimization problem considering a horizon of future instants, called prediction horizon T_f. According to the logic of the MPC, the optimization problem is solved at each sampling time τ_s to exploit the updated measures of the system, such as the state of charge of the batteries and the power exchanged by the cluster, recalculating each time the optimal control action over the entire prediction horizon. At this point, however, only the initial control action is implemented by the system, and the procedure is repeated at the next sampling instant using the updated measurements and reserves.

The C-MPC regulators are designed not to require the measurement of the instantaneously exchanged power from non-dispatchable local units, for example, network loads, while the measurement of the power exchanged between clusters is required. The C-MPC regulator can therefore estimate the aggregate disturbance acting on the ith cluster, defined $\widetilde{d}_i(t)$, as the difference between the measured net power of the cluster and the corresponding expected value, given by the predictions, plus the power changes requested by C-MPC at the previous control iteration. This is expressed as follows:

$$\begin{aligned}\widetilde{d}_i(t) = \bar{P}_{\text{net},i}(t) - P_{\text{net},i}(t) + \sum_{k \in \aleph_i^G} \Delta P_{G,ki}(t-1) \\ + \sum_{k \in \aleph_i^B} \Delta P_{B,ki}(t-1) + \Delta P_{DC,i}(t-1)\end{aligned} \quad (5)$$

where $\bar{P}_{\text{net},i}$ is the day-ahead scheduling of the power exchanged by the ith cluster, $P_{\text{net},i}$ is the AC net active power of the ith cluster, $\Delta P_{G,ki}$, $\Delta P_{B,ki}$ and $\Delta P_{\text{DC},i}$ are the active power variation of the kth generator, battery and DC interface of the ith cluster.

Thus, considering the disturbance and the power changes requested by the control at the previous iteration, (5) can be rewritten as:

$$\begin{aligned}P_{\text{net},i}(t) = \bar{P}_{\text{net},i}(t) + \sum_{k \in \aleph_i^G} \Delta P_{G,ki}(t-1) \\ + \sum_{k \in \aleph_i^B} \Delta P_{B,ki}(t-1) + \Delta P_{\text{DC},i}(t-1) - \widetilde{d}_i(t)\end{aligned} \quad (6)$$

Considering the ith cluster, the main objective of the C-MPC is to track $\bar{P}_{\text{net},i}(t)$ that is scheduled the day-ahead. This is performed considering on the overall prediction horizon $h \in T_N(t) = \{t, \ldots, t+N\}$, where $N = \frac{T_f}{\tau_s}$, and a reasonable small tolerance margin ρ, as follows:

$$-\rho \leq P_{\text{net},i}(h) - \bar{P}_{\text{net},i}(h) \leq \rho \quad (7)$$

Since the power trend of the cluster depends on the unknown future value of the disturbance, it is assumed that this is constant over the entire prediction horizon and that it is equal to the value

estimated at instant t based on the measurements available:

$$d_i(h) = \widetilde{d}_i(t) \ \forall h \in T_N(t) \tag{8}$$

The cost function of the C-MPC of the ith cluster is stated as indicated as follows:

$$\begin{aligned} J_i(t) = \sum_{h=t}^{N} \Big\{ & \gamma_{\mathrm{net}_i} \left(P_{\mathrm{net},i}(h) - \bar{P}_{\mathrm{net},i}(h)\right)^2 \\ & + \gamma_{DC_i} \left(\Delta P_{DC,i}(h)\right)^2 + \sum_{k \in \aleph_i^D} \gamma_{G,\mathrm{ki}} \left(\Delta P_{G,ki}(\mathrm{h})\right)^2 \\ & + \sum_{k \in \aleph_i^B} + \gamma_{B,\mathrm{ki}} \left(\Delta P_{B,k}(\mathrm{h})\right)^2 \Big\} + \gamma_{SOC_i}^{\mathrm{end}} \sum_{k \in \aleph_i^B} \Delta E_{B,ki}^2 (t + \mathrm{N}) \end{aligned} \tag{9}$$

where γ_{net_i}, γ_{DCi}, $\gamma_{G,\mathrm{ki}}$, $\gamma_{B,\mathrm{ki}}$ and $\gamma_{SOC_i}^{\mathrm{end}}$ are positive non-null weights. In this cost function are penalized the variation of power of both generators and batteries, and the error in the tracked power. In case of reserves' shortages, the C-MPC can act on the DC power requests and the battery energy variation at the end of optimization horizon. Therefore, $\Delta P_{\mathrm{DC},i}$ and $\Delta E_{B,ki}$ are used as slack variables with $\gamma_{\mathrm{DC}_i}, \gamma_{\mathrm{SOC}_i}^{\mathrm{end}} > \gamma_{\mathrm{net}_i}, \gamma_{G,\mathrm{ki}}, \gamma_{B,\mathrm{ki}}$. At each time instant t, the C-MPC of the ith cluster must solve the following optimization problem to compute the optimal variables at each time instant t

$$\begin{aligned} & \min_{\Delta P_{D,ki}, \Delta P_{B,ki}, \Delta P_{DC,i}} \quad J_i(t) \\ & \text{subject to } (2), (3), (4), (6), (7), (8). \end{aligned} \tag{10}$$

2.3 | Supervisor module

In the case of the local power sources are not able to locally compensate for the variability, a power request is sent to the supervisor module which provides for the solution of an optimization problem, executed immediately after the execution of the C-MPC. This procedure is performed only if at least one C-MPC has sent a support request. It is worth noting that the supervisor level must be executed within a C-MPC sampling time. The supervisor's objective is to support the clusters that require power, directing it from those clusters that have availability of power, acting on the controllable interfaces of the DC multi-terminal network and transferring power among different areas of the network. In this way, the supervisor ensures that the C-MPCs are always able to operate autonomously, since it does not interfere with their action, and ensures that the variability of loads and RESs is compensated in each section of the network. The solution of the supervisor module does not involve significant computational issues, since it is a matter of solving a simple static optimization problem, while the complexity is mostly dealt at the C-MPC level. The constraints of the supervisor problem are detailed in (11)–(16), where (11) expressed the total power variation of the ith interface, that is composed by the terms $\Delta P_{\mathrm{DC}i}^{C\,*}(t)$ and $\Delta P_{\mathrm{DC}i}^{\mathrm{sup}}(t)$, where the former is the request of the cluster (obtained by solving (10)) and the latter is an optimization variable.

$$\Delta P_{\mathrm{DC}i}(t) = \Delta P_{\mathrm{DC}i}^{C\,*}(t) + \Delta P_{\mathrm{DC}i}^{\mathrm{sup}}(t) \tag{11}$$

During the operation of the system, to avoid any instability, the total power across the multiterminal DC grid must be equal to zero:

$$\sum_{i=1}^{n_c} \Delta P_{\mathrm{DC}i}(t) = 0 \tag{12}$$

The fulfilment of the DC power request from the ith cluster is achieved through the following constraints, that considers, through the term $\sigma_i(\mathrm{t}) = sign(\Delta P_{\mathrm{DC}i}^{C\,*}(t))$, the direction of the power request:

$$\sigma_i(\mathrm{t})\, \Delta P_{\mathrm{DC}i}(t) \geq \sigma_i(\mathrm{t})\, \Delta P_{\mathrm{DC}i}^{C\,*}(t) \tag{13}$$

The action of the supervisor has an influence on each cluster reserve. So, the clusters' reserves $R_i^{C\downarrow}(t)$ and $R_i^{C\uparrow}(t)$ can be calculated after the supervisor action as following:

$$\begin{aligned} R_i^{C\downarrow}(t) &= R_i^{C\downarrow *}(t) + \Delta P_{\mathrm{DC},i}^{\mathrm{sup}}(t) \\ R_i^{C\uparrow}(t) &= R_i^{C\uparrow *}(t) + \Delta P_{\mathrm{DC},i}^{\mathrm{sup}}(t) \end{aligned} \tag{14}$$

To limit the use of the reserves of each cluster, it has been introduced the slack variable $\Delta\varphi_i$, that is bounded between 0 and $\bar{\varphi}$.

$$0 \leq \Delta\varphi_i \leq \bar{\varphi} \tag{15}$$

To avoid shortage of clusters' reserves the threshold are so reduced using the slack variable.

$$\begin{aligned} R_i^{C\downarrow}(t) &\leq (\bar{\varphi} - \Delta\varphi_i)\, R_i^{C\downarrow *}(t) \\ R_i^{C\uparrow}(t) &\geq (\bar{\varphi} - \Delta\varphi_i)\, R_i^{C\uparrow *}(t) \end{aligned} \tag{16}$$

The cost function to be minimize by the supervisor can be formulated as:

$$\begin{aligned} J_s(t) = \sum_{i=1}^{n_c} \Big\{ & \gamma_p\, \Delta P_{\mathrm{DC},i}(t)^2 + \gamma_\varphi\, \Delta\varphi_i^2 \\ & + \gamma_r \left(\Delta P_{\mathrm{DC},i}(t) - \Delta P_{\mathrm{DC},i}(t-1)\right)^2 \Big\} \end{aligned} \tag{17}$$

where $\Delta P_{\mathrm{DC},i}$ is the power variation of the ith DC interface, $\Delta\varphi_{\mathrm{i}}$ is a slack variable used to respect power reserves thresholds and $\gamma_p, \gamma_\varphi, \gamma_r$ are positive non-null weights.

Therefore, the optimization problem that must be solved at the supervisory level can be stated as follows:

$$\begin{aligned} & \min_{\Delta P_{\mathrm{DC}\,i}, \Delta P_{\mathrm{DC}\,i}^{\mathrm{sup}}, \Delta\varphi_i, \forall i \in \{1, \ldots, n_c\}} \quad J_s(t) \\ & \text{subject to, } \forall i \in \{1, \ldots, n_c\}, (11), (13), (14), (15), (16), \text{and } (12). \end{aligned} \tag{18}$$

As evident, the supervising optimization problem (18) includes both the local optimization variables, that is, $\Delta P_{\mathrm{DC}\,i}$, $\Delta P^{\mathrm{sup}}_{\mathrm{DC}\,i}$ and $\Delta\varphi_i$, and local constraints, that is, (11), (13), (14), (15), (16), related to each single cluster, whereas (12) is a coupling constraint that interconnects all the clusters' variables.

This peculiar structure of the supervisory optimization problem enables to solve it using distributed optimization algorithms based on the duality theory. Therefore, differently from [21], a completely distributed implementation of the supervisor [24] is here proposed, which allows to obtain considerable advantages from the point of view of flexibility and scalability of the control system. Thus, the goal is to no longer use a centralized supervisor, but to replace it with a distributed algorithm that allows direct interaction between clusters, submitting support requests when necessary. Each distributed module of the supervisory level is designed to controls the corresponding AC/DC interface between the cluster and the DC multi-terminal network, to define the necessary power exchanges. Furthermore, the implemented algorithm must allow communication, even partial, among the clusters, so that each cluster interacts only with its directly connected neighbours and does not need to communicate with all the clusters in the network.

An algorithm that combines consensus techniques and distributed optimization based on duality was used. The algorithm used is called the dual consensus alternating direction method of multipliers (DC-ADMM) [25]. Hereafter, a brief overview for the derivation of such algorithm is provided, but we refer the reader to [26] for more details on the different mathematical steps.

For the sake of clarity, let us firstly compact the local optimization variables of each ith cluster as $x_i = [\Delta P_{\mathrm{DC}\,i}, \Delta P^{\mathrm{sup}}_{\mathrm{DC}\,i}, \Delta\varphi_i]$ and a generic set X_i where the local variables x_i must be included to respect the local constraints (11), (13), (14), (15), (16), that is, $x_i \in X$. Also define the following matrix:

$$E = \begin{bmatrix} 1 & 0 & 0 \\ 0 & 0 & 0 \\ 0 & 0 & 0 \end{bmatrix}$$

and introduce the following cost function for each ith cluster:

$$f_i\left(x_i\left(t\right)\right) = \gamma_p\,\Delta P_{\mathrm{DC},i}(t)^2 + \gamma_\varphi\,\Delta\varphi_i^2 + \gamma_r\left(\Delta P_{\mathrm{DC},i}\left(t\right) - \Delta P_{\mathrm{DC},i}\left(t-1\right)\right)^2. \quad (19)$$

Hereafter, the time index t is removed for the sake of clarity. This implies that the centralized supervisory optimization problem (18) can be compactly rewritten as

$$\begin{aligned} \min_{x_i,\,\forall i\,\in\,\{1,\ldots,n_c\}} \quad & \sum_{i=1}^{n_c} f_i\left(x_i\right) \\ \text{subject to } & x_i \in X_i, \forall i \in \{1,\ldots,n_c\}, \\ & \sum_{i=1}^{n_c} E\,x_i = 0 \end{aligned} \quad (20)$$

The optimization problem (20) is named as *primal problem* and it is a convex optimization problem. Also consider a communication network among the grid clusters, defined through the unoriented graph $G(C,E)$ where the set $C = \{1,\ldots,n_c\}$ whereas $E \subseteq C \times C$ includes the communication links among the clusters. The communication graph is assumed to be connected, that is, there are not isolated clusters or group of clusters. Moreover, let us define with $C_i = \{j \in C |\ (i,j) \in E\}$ the set of neighbouring clusters of the ith cluster.

Given the peculiar structure of the primal problem, where there is a separable cost function, separable local constraints and a coupling constraint, dual-based optimization problems can be effectively applied. To do that, define firstly the Lagrangian function of the problem as:

$$L\left(x_1,\ldots,x_{n_c}\right) = \sum_{i=1}^{n_c} f_i\left(x_i\right) + \lambda \sum_{i=1}^{n_c} E\,x_i \quad (21)$$

where the coupling constraint of problem (20) is relaxed using the dual variable λ. The dual variable acts as a weight to enforce the respect of the coupling constraint. At this stage, the dual problem can be defined as:

$$\max_{\lambda} \sum_{i=1}^{n_c} \min_{x_i \in X_i} f_i\left(x_i\right) + \lambda\,E\,x_i \quad (22)$$

As known in duality optimization theory, if some mild assumptions are respected (e.g. convexity of the primal problem), the optimal solutions achieved by the primal and dual problem coincide. Thus, defining the function $\phi_i\left(\lambda\right) = -\min_{x_i \in X_i} f_i(x_i) + \lambda\,E\,x_i$, the dual problem (21) can be rewritten as

$$\min_{\lambda} \sum_{i=1}^{n_c} \phi_i\left(\lambda\right). \quad (23)$$

Now, exploiting that the communication graph is connected, it can be shown that the optimization problem (23) is equivalent to:

$$\begin{aligned} \min_{\lambda_1,\ldots,\lambda_{n_c}} \quad & \sum_{i=1}^{n_c} \phi_i\left(\lambda_i\right) \\ \text{subject to,} \quad & \lambda_i = \lambda_j, \forall i \in C, \forall j \in C_i \end{aligned} \quad (24)$$

where λ_i corresponds to the local copy of the dual variable λ for each ith cluster. The optimal solution of problem (24) implies that all the agents reach a consensus on the local copies of the dual variables, which in the end will correspond to the optimal solution of (22). As discussed in detail in [26], the algorithm to solve the optimization problem (24) is fully distributed, and this is reported in Algorithm 1. As evident from Algorithm 1, the distributed supervisors act completely in parallel, solving steps 1–5. Moreover, the algorithm is iterative, and it is guaranteed to converge if the primal problem is convex and the

Algorithm 1 Dual consensus alternating direction method of multipliers

Initialize:
$k = 1, \lambda_i^0 = 0, p_i^0 = 0, c =$ tuning parameter.

Repeat until convergence is reached. $\forall i \in C^c$, in parallel, each distributed supervisor does
1. $x_i^k = \arg\min_{x_i \in X_i}$
$$\left\{ f_i(x_i) + \frac{c}{4|C_i|} \cdot \left\| \frac{1}{c}(E\,x_i) - \frac{1}{c}p_i^{(k-1)} + \sum_{j \in C_i}, \left(\lambda_i^{(k-1)} - \lambda_j^k\right) \right\|_2^2 \right\}$$
2. $\lambda_i^k = \frac{1}{2|C_i|}\left(\sum_{j \in C_i}\left(\lambda_i^{k-1} - \lambda_j^{k-1}\right) - \frac{1}{c}p_i^{k-1} + \frac{1}{c}\left(E\,x_i^k\right)\right)$
3. Send λ_i^k to the supervisors of all neighbouring clusters jth, with $j \in C_i$
4. $p_i^k = p_i^{k-1} + c\sum_{j \in C_i}\left(\lambda_i^k - \lambda_j^k\right)$
5. $k = k + 1$

communication graph among the clusters' supervisors is connected [26]. A local optimization problem is solved in step 1, considering local constraints, local cost functions and the local copies of the dual variables of the neighbouring clusters at the previous iteration $k-1$. Then, the local copy of the dual variables λ_i is updated in step 2 and then sent to the neighbouring clusters, so that they can solve step 1 at the next iteration. Finally, another local dual variable is updated, that is, p_i, which is not shared among the clusters' supervisors, and it serves to enforce consensus among the local copies of the dual variables λ_i, for $i \in C$.

As shown in the experimental results, despite being an iterative algorithm, the fully distributed layer can control and optimize the AC/DC power exchanges in reduced computational time given the fact that the supervisory optimization problem is static, while the dynamical complexity is mostly addressed by the low-level clusters regulators.

3 | EXPERIMENTAL SETUP

The experimental validation of the control functions presented in Section 2 was carried out through the distributed energy resources test facility (DER-TF) of RSE [27, 28], shown in Figure 2. This is a real low-voltage hybrid AC/DC microgrid where are installed RESs, dispatchable generators, storage systems and loads to perform experimental activities on DERs and smart grid solutions. This experimental microgrid covers an area of about 20,000 m^2, is interconnected to the MV grid by the means of an 800 kVA dedicated transformer (23 kV/400 V), has an overall capacity of 300 kW (active power) and 300 kVAr (reactive power) and can be reconfigured to realized different setups.

To carry out the tests, this hybrid AC/DC grid was divided into two clusters connected each other via an AC line and a DC link. The components of the network have been divided in such a way as to have a suitable distribution of the components in the two cells. The microgrid was in fact configured to have a cell made up of five distributed units with reduced power (22 kW of generation, 18 kW of load, 20 kWh of battery) and a second cell in which three distributed units with higher power are installed

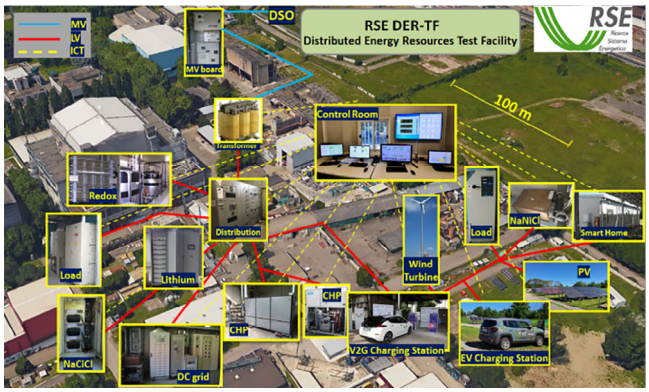

FIGURE 2 Schematic of the distributed energy resources test facility of RSE.

(90 kW load, 50 kW generation, 67 kWh battery). Each cell contains at least a source of disturbance (load or PV generation), a storage system, a controllable generator, and a direct current interface. A schematic of the system under test is presented in Figure 3, while the parameters of the components are collected in Table 1.

4 | EXPERIMENTAL RESULTS

During tests, the cluster control systems, C-MPC, are executed with a sampling time τ_s of 1 min and a prediction horizon T_f equal to 15 min. The supervision system is activated only on request of the cluster controllers that run every 1 min. Therefore, the supervisor can be activated at most every 1 min just in case some of the clusters do not have enough reserve.

4.1 | Evaluation of the best weight for the final SoC

In the C-MPC the weights of the slack variables in the objective function determine a different contribution of the storage systems present in the network and a consequent different action of the direct current interfaces. In particular, the weight assigned to the final state of charge in the prediction horizon, indicated with $\gamma_{\mathrm{SOC}_i}^{\mathrm{end}}$, is the one that most influences the action of the storage systems and consequently on the various dispatchable devices. To highlight the effect of this weight on the results, the results of three short-term tests carried out with three different values of the weight $\gamma_{\mathrm{SOC}_i}^{\mathrm{end}} = \{10000, 1000, 100\}$ and with the same values for the other weight $\gamma_{DC_i} = 200; \gamma_{\mathrm{net}_i} = 100; \gamma_{G,\mathrm{ki}} = 1; \gamma_{B,\mathrm{ki}} = 0.1$ are shown below.

The system was tested over a short-term test with power disturbances with respect to the load and photovoltaic forecasts that act on both clusters, as shown in Figure 4. During the tests, it is supposed that each cluster is operated to set to zero the power exchanged with the grid. The results of the test highlight that a high weight on $\gamma_{\mathrm{SOC}_i}^{\mathrm{end}}$ (Case1) reduces the use of the storage systems (nodes 3 and 12) and increases the use of other

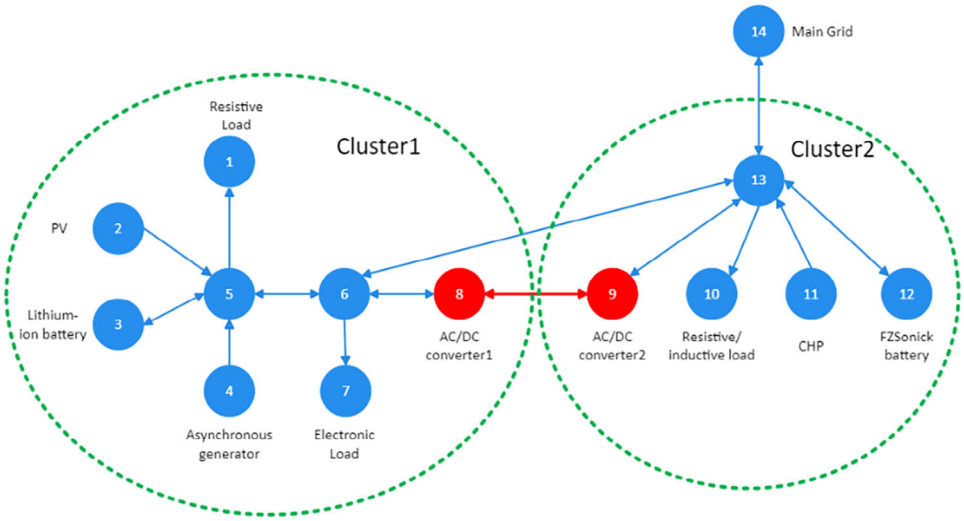

FIGURE 3 Schematic of the distributed energy resources test facility configuration during the test.

TABLE 1 Parameters of the components in the grid.

Cluster	Node number	Resource	$P_{min} \div P_{max}$ in kW	E_n in kWh	SOC in %
1	1	Resistive load	0 ÷ 16	–	–
1	2	Photovoltaic (PV) Generator	0 ÷ 17	–	–
1	3	Lithium-ion battery	−20 ÷ 20	20	10 ÷ 90
1	4	Asynchronous generator	0 ÷ 7.5	–	–
1	7	Electronic load	0 ÷ 12	–	–
1	8	AC/DC converter1	−100 ÷100	–	–
1	9	AC/DC converter2	−30 ÷ 30	–	–
1	10	Resistive/inductive load	0 ÷ 90	–	–
2	11	Combined Heat and Power (CHP) Generator	5 ÷ 50	–	–
2	12	FZSonick battery	−18 ÷ 18	67	10 ÷ 90

dispatchable resources as shown in Figures 5 and 6, where the asynchronous generator (node 4) and the CHP (node 11) have very high power excursions to compensate the power variations of loads and PVs. Furthermore, the control system makes extensive use of power exchange via the DC connections, modulating the power exchanged by the AC/DC interfaces. (nodes 8 and node 9) with high weight on the final SoC of the batteries.

However, a smaller weight for the slack variable $\gamma^{end}_{SOC_i}$ (Case3) leads to a greater use of the batteries, and a more sustained deviation of the state of charge compared to the initial value, as shown in Figure 7. This choice of parameters ensures that power exchanges take place between cells via the DC lines and that the C-MPC control systems fully use their internal resources to compensate for unexpected variations.

The choice of weights significantly influences how the cluster controllers manage internal resources. Therefore, it is possible to decide whether to favour greater use of storage systems or prefer that these are preserved by resorting to greater requests between cells to compensate for variability.

4.2 | Test results

To verify the performances and the abilities of the control system to compensate disturbances, both at generation and demand level, the system was tested over a full day where there are power disturbances with respect to the load and photovoltaic forecasts that act on both clusters into which the DER-TF has been divided, as evident from Figure 8. Moreover, it is supposed that each cluster is operated to set to zero the power exchanged with the grid. During the test has been used the weights presented in the previous section. Moreover, to overcome the excessive variation of SoC at the end of the day, instead of using a constant weight γ^{end}_{E}, it was used a weight that gradually increases over time. The following results has been achieved using a weight for the lithium battery equal to $\gamma^{end}_{E} = t^2$ and for the FZSonick battery equal to $\gamma^{end}_{E} = 0,1t^2$. In this condition, the batteries will provide their contribution throughout the entire day, while towards the end of the day they will tend to provide an increasingly lower contribution

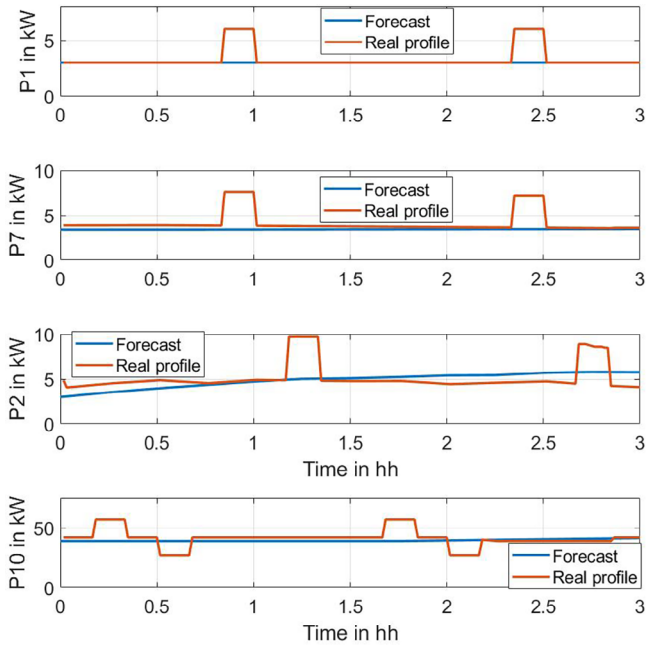

FIGURE 4 Trend of the forecast and real profile of loads and PV generation. P1, resistive load; P7, electronic load; P2, PV generation; P10, resistive/inductive load during test with different $\gamma_{SOC_i}^{end}$.

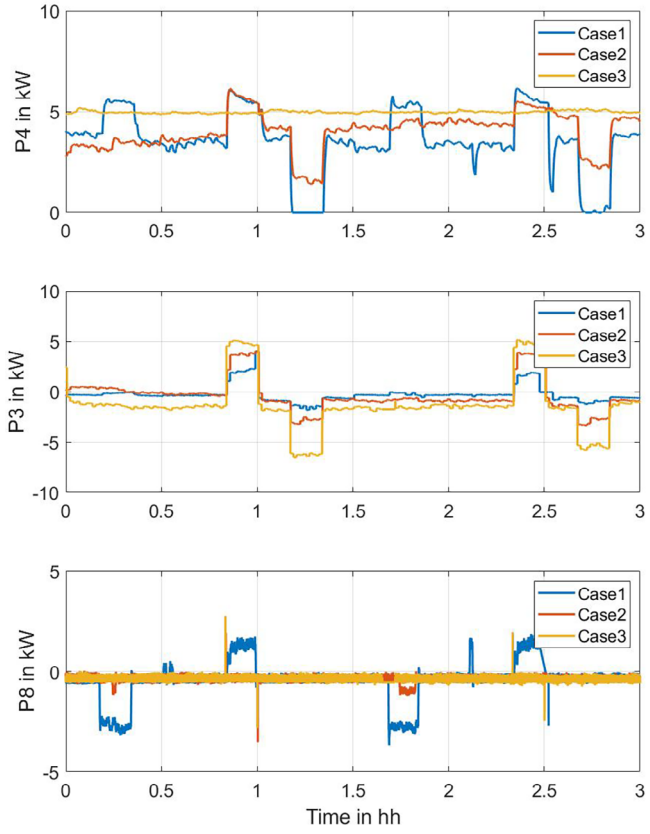

FIGURE 5 Trend of the power exchanged by the controllable resources in the cluster1. P4, asynchronous generator; P3, lithium-ion battery; P8, AC/DC converter1 during test with different $\gamma_{SOC_i}^{end}$.

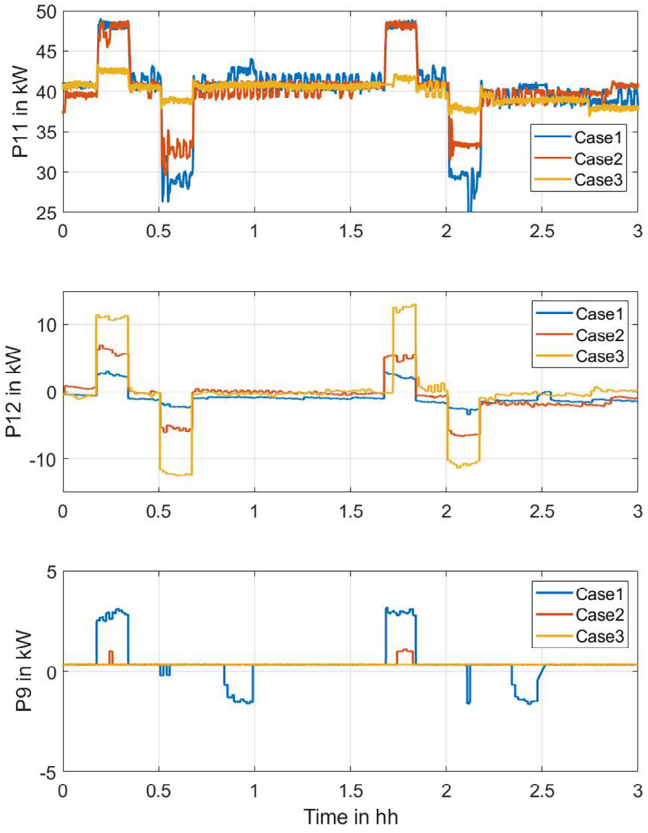

FIGURE 6 Trend of the power exchanged by the controllable resources in the cluster2. P11, CHP; P12, FZSonick battery; P9, AC/DC converter1 during test with different $\gamma_{SOC_i}^{end}$.

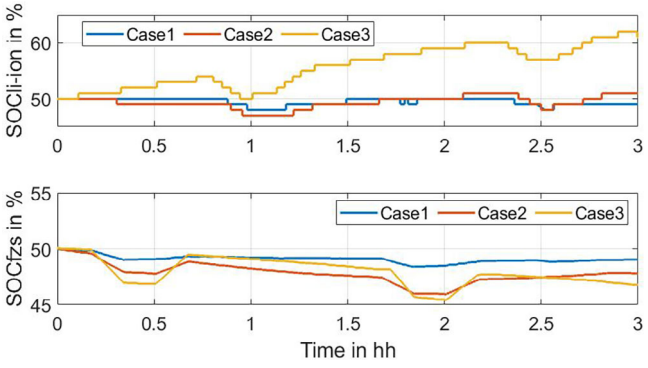

FIGURE 7 Trend of the SOC of the batteries during test with different $\gamma_{SOC_i}^{end}$.

which guarantees the restoration of the state of charge to the programmed value and equal to 50% for this test.

Despite the presence of disturbances and the wrong forecasts, the proposed control architecture can promptly coordinate the power outputs of controllable resources such that the power exchanges of clusters with the main grid, as shown in Figure 9, always remain close to zero, recording short, more sustained power peaks given by the significant variations in load

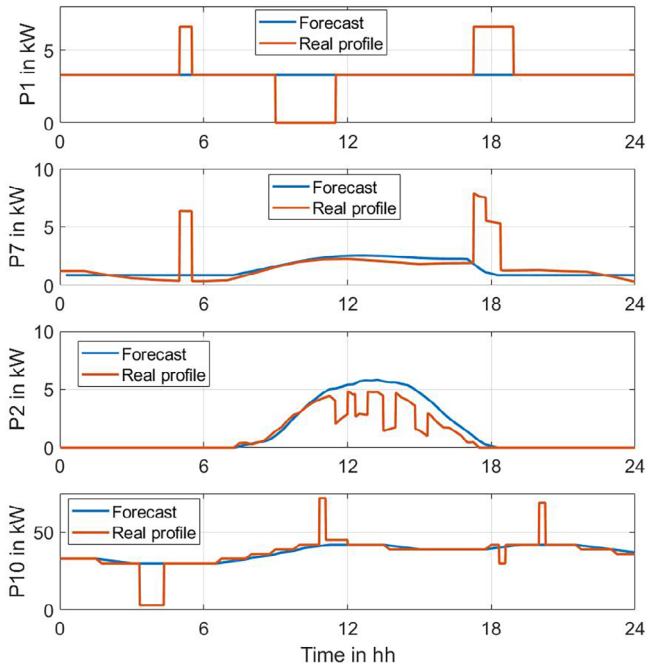

FIGURE 8 Trend of the forecast and real profile of loads and PV generation. P1, resistive load; P7, electronic load; P2, PV generation; P10, resistive/inductive load.

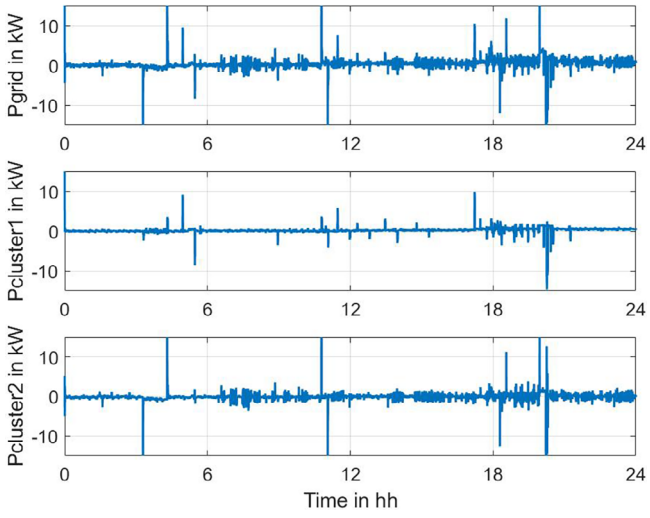

FIGURE 9 Trend of the power exchanged with the grid and with the two clusters.

and RES. This result is achieved thanks to the modulation of the dispatchable resources of each cluster. Figures 10 and 11 show how cluster control systems decide to modulate local resources to compensate for variations.

The test shows that if clusters can satisfy load or generation variation, the power requested to the DC converter is equal to zero. However, if clusters are unable to satisfy the variations, due to the reaching of the technical limits of the controllable resources, the clusters themselves can make up for the lack of resources by acting on DC interfaces.

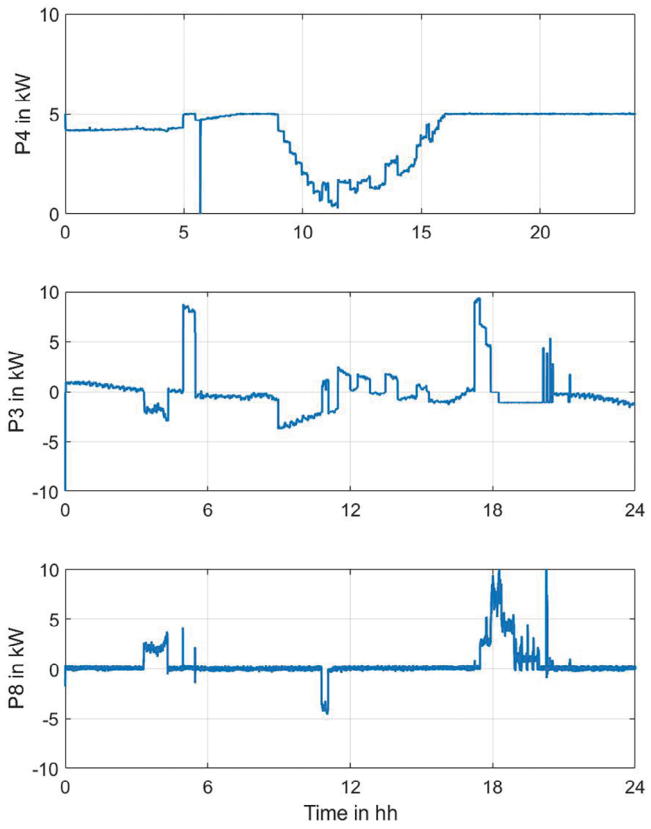

FIGURE 10 Trend of the power exchanged by the controllable resources in the cluster1. P4, asynchronous generator; P3, lithium-ion battery; P8: AC/DC converter1.

Given the significant entity of the variations (see Figure 10), it can be seen how the control systems make extensive use of power exchanges through the DC converters. For example, the significant decrease in the absorbed power of cluster 2 around 4:00, which involves the sudden decrease in the power supplied by the CHP and by the FZSonick battery, which, however, reach their technical minima as indicated in Figure 11. For this reason, the C-MPC of cluster 2 requires support from that of cluster 1, which absorbs, via the lithium battery, the additional power necessary to guarantee zero exchange with the grid. An opposite case can be seen between 17:00 and 19:00, when the large peaks acting on loads of cluster 1 are compensated through a power transfer from cluster 2 to cluster 1 over the DC link.

Finally, Figure 12 shows that, despite the presence of time-varying disturbances to be compensated, batteries SOC are maintained inside the prescribed bounds by the proposed control architecture [23] and thanks to the use of a weight γ_E^{end} that gradually increases over time, the SoC of both the battery is restored to the programmed value equal to 50%.

4.3 | Comparison between centralized and distributed supervisor

In the end, it is interesting to note the performance of the distributed supervisor and compare it with the performance of a

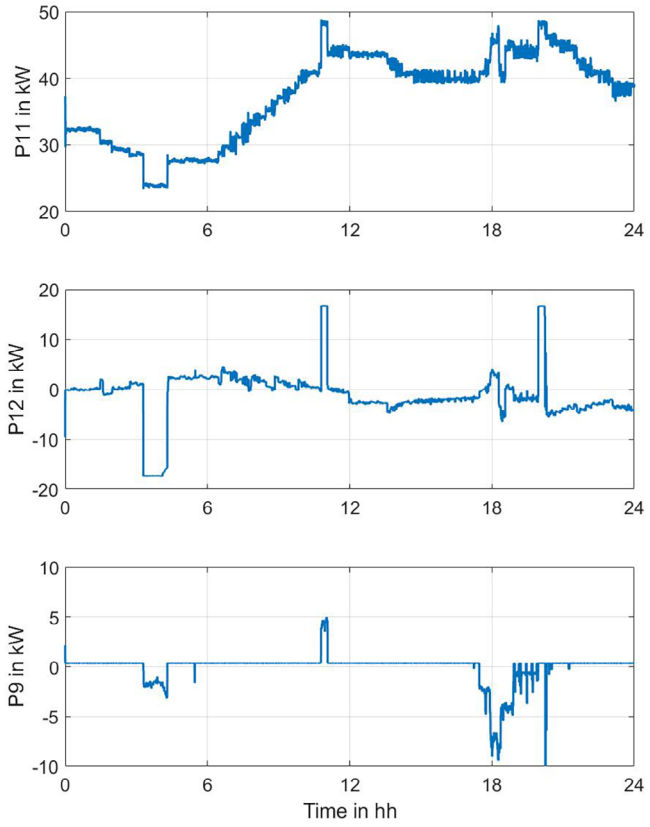

FIGURE 11 Trend of the power exchanged by the controllable resources in the cluster2. P11, CHP; P12, FZSonick Battery; P9, AC/DC converter1.

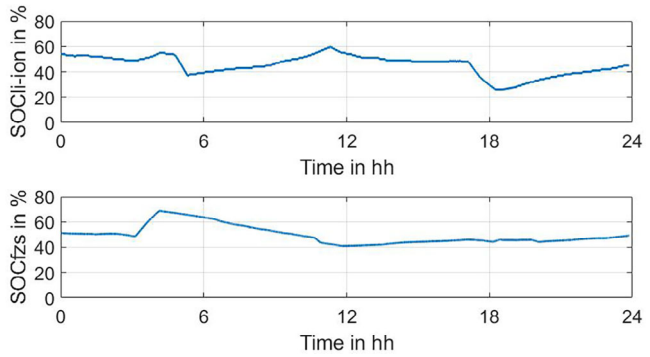

FIGURE 12 Trend of the SOC of the batteries.

centralized supervisor. The control system with a distributed supervisor, despite its high scalability and flexibility in managing an indefinite number of clusters, has the disadvantage of being an iterative algorithm. However, as shown in Figure 13, the number of iterations is limited and less than 30 during the entire test. Although the number of iterations is limited, this determines that the computation times of the distributed supervisor are higher than that of the centralized one, as shown in Figure 14. However, these are always negligible computing times, given that the centralized reaches peaks of 0.25 s while the distributed supervisor reaches a maximum of 4 s. However, these computation times are much lower than the operating

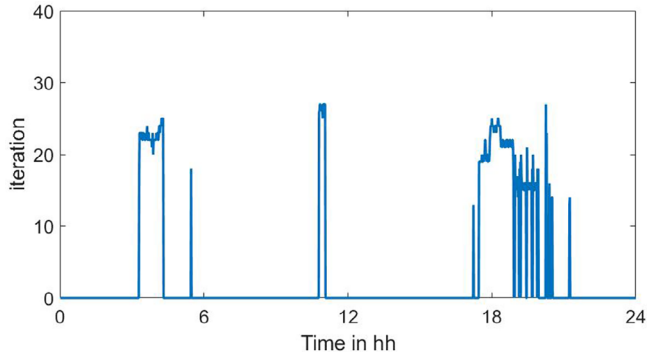

FIGURE 13 Number of iterations to reach the convergence of the distributed supervisor.

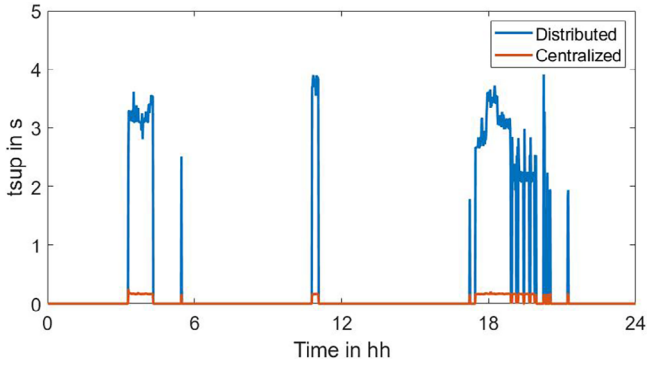

FIGURE 14 Comparison between the time to compute the supervisor problem in case of distributed and centralized control.

times of the controller which is executed every minute. From these results, the distributed controller does not have any impact on the performance of the overall system. It is also worth noting that the advantages of a distributed supervisor are more appreciated when larger networks are controlled, with many clusters. In fact, in that case, the computation times of the centralized supervisor would increase considerably with the increase in the optimization variables, while a distributed supervisor would be slightly affected by the increase in agents given that they always solve optimization problems in parallel.

5 | CONCLUSION

The experimental activity conducted and shown in this paper has allowed an experimental validation of the control techniques for AC/DC distribution networks divided into clusters. As evident, the developed control architecture enables optimal management of the grid clusters even in the case of high forecast errors. The main advantages of the proposed solution are its scalability and prompt control action to compensate for unexpected unbalances. The control system through its two-level structure allows high degrees of freedom, making it possible to control even very large distribution networks, suitably partitioned into clusters. The control architecture is structured in two layers. The lower-level control system, called C-MPC is

decentralised and considers the optimization of each grid cluster. On the other hand, the high supervisory layer, which is fully distributed, optimizes the power exchanges among the clusters without even the need for a central entity. The proposed architecture shows enhanced scalability properties, given that the agents solve their optimization problems in parallel and the computation time, therefore, is not influenced by their number. The potentialities of the proposed method are confirmed by the test campaign, run on a real hybrid AC-DC experimental benchmark. Different future directions can be employed for this work. First, the approach can be improved by considering electrical grid systems without DC multi-terminal grids by properly synchronizing the net power exchange of each grid area. Moreover, another interesting future development is the application of this control strategy to other energy contexts, for example in the presence of water distribution networks, district heating networks and gas networks. The scalable control of energy clusters exchanging flexibilities could be very useful for managing the interaction of different energy vectors, to improve their efficiency and maximize their energy flexibility in support of the overall energy system.

AUTHOR CONTRIBUTIONS

Riccardo Lazzari: Conceptualization; methodology; supervision; validation; writing—original draft. **Alessio La Bella**: Conceptualization; formal analysis; methodology; software; writing—review and editing.

ACKNOWLEDGEMENTS

This work has been financed by the Research Fund for the Italian Electrical System under the Three-Year Research Plan 2022–2024 (DM MITE n. 337, 15.09.2022), in compliance with the Decree of April 16th, 2018.

CONFLICT OF INTEREST STATEMENT

The authors declare no conflicts of interest.

DATA AVAILABITY STATEMENT

Data available on request from the authors.

ORCID

Riccardo Lazzari https://orcid.org/0000-0002-3441-4784

REFERENCES

1. Barragan-Villarejo, M., Martinez-Ramos, J., Garcia-Lopez, P., Marano-Marcolini, A., Maza-Ortega, J.M.: Improving the controllability of microgrids through DC links. In: Proceedings of the 2018 IEEE International Energy Conference (ENERGYCON). IEEE, Piscataway, NJ (2018)
2. Bucher, M.K., Wiget, R., Andersson, G., Franck, C.M.: Multiterminal HVDC networks what is the preferred topology? IEEE Trans. Power Delivery 29, 406–413 (2014)
3. Negra, N.B., Todorovic, J., Ackermann, T.: Loss evaluation of HVAC and HVDC transmission solutions for large offshore wind farms. Electr. Power Syst. Res. 76, 916–927 (2006)
4. Dierckxsens, C., Srivastava, K., Reza, M., Cole, S., Beerten, J., Belmans, R.: A distributed DC voltage control method for VSC MTDC systems. Electr. Power Syst. Res. 82, 54–58 (2012)
5. Burstein, A., Cuk, V., de Jong, E.: Determining potential capacity gains when repurposing MVAC cables for DC power transportation. CIRED—Open Conf. Proc. J. 2017(1), 1691–1694 (2017)
6. Zhang, L., et al.: Converting AC distribution lines to DC to increase transfer capacities and DG penetration. IEEE Trans. Smart Grids 10(2), 1477–1487 (2019)
7. Larruskain, D., Zamora, I., Abarrategui, O., Aginako, Z.: Conversion of ac distribution lines into dc lines to upgrade transmission capacity. Electr. Power Syst. Res. 81, 1341–1348 (2011)
8. Krahmer, S., Rupp, S., Adam, R., Backhaus, K., Hildmann, C., Nilges, M., Schegner, P.: Conversion of existing AC into DC cable links in distribution grids: Benefits and challenges. In: Proceedings of the ETG-Congress, pp. 1–6. IEEE, Piscataway, NJ (2021)
9. Shekhar, A., et al.: Grid capacity and efficiency enhancement by operating medium voltage AC cables as DC links with modular multilevel converters. Electr. Power Energy Syst. 93, 479–493 (2017)
10. Marano-Marcolini, A., Romero-Ramos, E., Gomez-Exposito, A., Ortega, J.M., Martinez-Ramos, J.: Enhancing the integration of renewable sources in distribution systems using dc-links. In: Proceedings of the 2009 IEEE PES/IAS Conference on Sustainable Alternative Energy (SAE). IEEE, Piscataway, NJ (2009)
11. Hirth, L., Ziegenhagen, I.: Balancing power and variable renewables: Three links. Renewable Sustainable Energy Rev. 50, 1035–1051 (2015)
12. Lasseter, R.H., Piagi, P.: Microgrid: A conceptual solution. In: Proceedings of the IEEE Power Electronics Specialists Conference, pp. 1–5. IEEE, Piscataway, NJ (2004)
13. Maciejowski, J.M.: Predictive Control: With Constraints. Pearson Education, London (2002)
14. Scattolini, R.: Architectures for distributed and hierarchical model predictive control–A review. J. Process Control 19(5), 723–731 (2009)
15. Hug-Glanzmann, G.: Coordination of intermittent generation with storage, demand control and conventional energy sources. In: Proceedings of the 2010 IREP Symposium Bulk Power System Dynamics and Control—VIII (IREP), pp. 1–7. IEEE, Piscataway, NJ (2010)
16. Raimondi Cominesi, S., Farina, M., Giulioni, L., Picasso, B., Scattolini, R.: A two-layer stochastic model predictive control scheme for microgrids. IEEE Trans. Control Syst. Technol. 26(1), 1–13 (2018)
17. Feng, X., Shekhar, A., Yang, F., Hebner, R.E., Bauer, P.: Comparison of hierarchical control and distributed control for microgrid. Electr. Power Comp. Syst. 45(10), 1043–1056 (2017)
18. Nowak, S., Wang, L., Metcalfe, M.S.: Two-level centralized and local voltage control in distribution systems mitigating effects of highly intermittent renewable generation. Int. J. Electr. Power Energy Syst. 119, 105858 (2020)
19. Baker, K., Guo, J., Hug, G., Li, X.: Distributed MPC for efficient coordination of storage and renewable energy sources across control areas. IEEE Trans. Smart Grid 7, 992–1001 (2016)
20. Molzahn, D.K., et al.: A survey of distributed optimization and control algorithms for electric power systems. IEEE Trans. Smart Grid 8(6), 2941–2962 (2017)
21. Bonassi, F., La Bella, A., Lazzari, R., Sandroni, C., Scattolini, R.: Supervised control of hybrid AC-DC grids for power balance restoration. Electr. Power Syst. Res. 196, 107107 (2021)
22. La Bella, A., Klaus, P., Ferrari-Trecate, G., Scattolini, R.: Supervised model predictive control of large-scale electricity networks via clustering methods. Optim. Control. Appl. Methods 43(1), 44–64 (2022)
23. Lazzari, R., Bella, A.L.: Optimal distributed control of hybrid AC/DC grids. In: Proceedings of the 2023 International Conference on Clean Electrical Power (ICCEP), pp. 571–578. IEEE, Piscataway, NJ (2023)
24. La Bella, A., Bonassi, F., Klaus, P., Scattolini, R.: A fully distributed control scheme for power balancing in distribution networks. IFAC-PapersOnLine 53(2), 13178–13183 (2020)
25. Chang, T.-H., Hong, M., Wang, X.: Multi-agent distributed optimization via inexact consensus ADMM. IEEE Trans. Signal Process. 63(2), 482–497 (2014)
26. Chang, T.: A proximal dual consensus ADMM method for multi-agent constrained optimization. IEEE Trans. Signal Process. 64, 3719–3734 (2016)

27. Sandroni, C., Verga, M., Lazzari, R., Fantini, M., Sacchi, M., Prandoni, V.: RSE's microgrid: A facility for research, development and testing of future distributed generation and microgrid technologies. In: Proceedings of the AEIT International Annual Conference, pp. 1–6. IEEE, Piscataway, NJ (2016)
28. Ronchegalli, D., Lazzari, R.: Development of the control strategy for a direct current microgrid: A case study. In: Proceedings of the AEIT International Annual Conference. IEEE, Piscataway, NJ (2016)

How to cite this article: Lazzari, R., La Bella, A.: Distributed multi-layer control of hybrid AC/DC grids: Design and experimental validation. IET Renew. Power Gener. 18(Suppl. 1), 4414–4425 (2024). https://doi.org/10.1049/rpg2.13161